1. Unpulsed magnetospheric emission, and PWN searches

In this section, we will search for emission in the phase range between the peaks of the pulsar's light curve. This potential DC emission could originate in the pulsar's winds, from inside the pulsar's magnetosphere, or the emission could be spatially coincidental but physically unrealted to the pulsar.

The GeV emission in the off-peak from LAT-detected pulsars has been studied in several previous publications. In particular, the spatially-extended Vela X pulsar wind nebula has been detected by the LAT in the off-peak phase region of the Vela pulsar (Ackermann et al. 2011) and the Crab nebula has been detected by the LAT (Abdo et al. 2010b). Surprisingly, this GeV emission from the Crab nebula was found to be variable in time (Abdo et al. 2011).

Most prominently, a dedicated analysis was performed using LAT data of the off-peak emission of 54 LAT-detected pulsars using 16 months of survey observations (Ackermann et al. 2011). The search discovered ten pulsars wich significant off-peak emission. Along with Vela X and the Crab nebula, the search discovered a source coincident with the TeV source HESS J1023-575 in the off-peak window of PSR J1023-5746. In addtion, four of hte other regions showed a significantly cutoff pulsar-like spectrum and are suspected to be be of magnetospheric origin.

We expand upon this previous work by searching in the off-peak region of all 107 pulsars presented in this catalog. In addition to the larger list of pulsars, in this earch we use an expanded data set, a larger energy range, and an improved analysis method.

1.1. Off-peak Phase Selection

To study the off-peak emission of LAT-detected pulsars, we first developed a systematic method for defining the off-peak emission. The primary constraint for this method was that it was systematic, computationally efficient, and model independent.

The method we developed proceeds by deconstructing the pulsar's phaseogram into a simple representation using the Bayesian Blocks algorithm as described in Jackson et al. (2005). To produce Bayesian Blocks on a peroid phaseogram, we applied the blocks instead to the data from a phase of -1 to 2 and then selected only the block interval from 0 to 1.

To find an idea off-peak region, we first optimized the pulsar phaseogram by varying the minimum energy and radius of the included photons to optimize the H-test. We then selected the lowest Baysian block to be the off-peak emission, and removed 10% of the emission from either side of the block to avoid any potential pulsed contamination near the boundaries.

There is one free parameter in the Baysian Block algorithm called $\mathrm{ncp}_{\mathrm{prior}}$ which modifies the probability that the algorithm dividing a block into smaller intervals. For our situation, we found that setting $\mathrm{ncp}_{\mathrm{prior}} = 8$ provided robust against the Baysian Block decomposition containing unphysically small blocks. In a few situations, the algorithm decomposed the phaseogram into one block and in these situations we reduced the $\mathrm{ncp}_{\mathrm{prior}}$ until we found an off-peak region.

In some situations, there could be two well defined off-peak regions between two peaks. In situations were the second lowest Baysian block was consistent with the first block (at the 1% confidence level) and when the second block contained at least half as much phase as the first block, we included the two phase ranges in the off-peak defintion.

Figure Figure 1 shows the energy-and-radius optimized light curve and the off-peak selection for a representative sample of pulsars.

1.2. Off-peak Analysis Method

We develope a procedure for characterizing any emission found in off-peak phase internals for the pulsars in this catalog. This proceure used both the spectral and spatial characteristics of any observed emission to determine the physical origin of the emission.

Pulsar wind nebula are expected in many cases to be spatially extended. For example, Vela X and HESS J1825-137 are PWN that have been observed by the LAT to be spatially extended (Ackermann et al. 2011; Grondin et al. 2011). On the other hand, not all pulsar wind nebula are expected to be significantly spatially resolved at GeV energies due to the finite instrument resolution of the LAT. For example, the Crab nebula appears as a point-like source in the LAT but is distinuished in the off-peak from the Crab pulsar by its hard spectrum for $\mathrm{E} \gtrsim 1$ GeV. (Abdo et al. 2010b).

On the other hand, a previous analysis by the Fermi LAT collaboration found seven off-peak regions to have significant emission which is point-like in nature that is characterized by a pulsar-like cutoff spectrum (Ackermann et al. 2011). We can thefore use either spatial extension or significant emission at high energy to distinguish the PWN scenario and point-like emission with a cutoff spectrum to distingiugh the pulsar scenario.

To perform this test, we used the likelihood fitting pacakge `pointlike` to study the spatial character of emission in the off-peak regions and `gtlike` in binned model to study the spectral character of the emission. These tools provide complementary features and this method is very similar to the approach used in the second LAT catalog (Nolan et al. 2012)

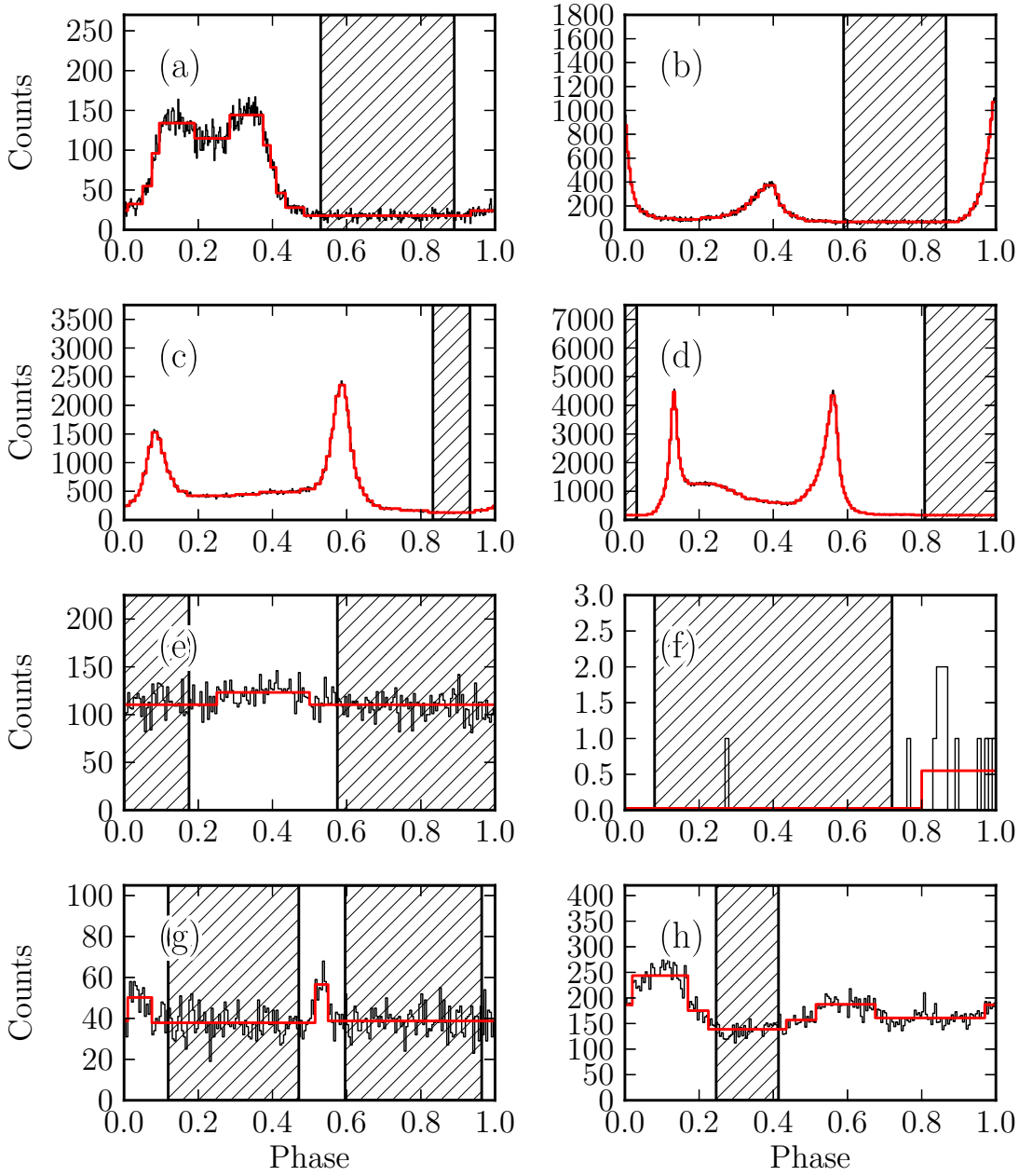

Fig. 1.— The phaseogram and off-peak selection for (a) PSRJ0007+7303, (b) PSRJ0534+2200, (c) PSRJ0633+1746, (d) PSRJ0835-4510, (e) PSRJ1702-4128, (f) PSRJ1747-4036, (g) PSRJ1801-2451, and (h) PSRJ2021+4026. The black hisotgram represnets the energy-and-radius optimized phaseogram. The gray lines (colored red in the electronic version) represent the Baysian block decomposition of the pulsar light curves. The hatched regions represent the off-peak region selected by this method.

and a followup search for spatially extended sources (Lande et al. 2012).

For this analysis, we build a model of the sky consistent with the second LAT catalog. We included as background sources all nearby sources from the second and used the same background model as the catalog (Nolan et al. 2012). Our analysis energy range varied from 100 MeV to 316 GeV. For this analysis, we removed all of the on-peak photons before binning the data and scaled the exposure to fit the all-phase flux assuming constant emission with phase.

With this model of the sky, we used fit an assumed source in the off-peak emission. First, we assumed the potential emission to have a point-like spatial model and (unless otherwise noted) a power-law spectral model. We used `pointlike` to fit the position of the off-peak region following the procedure described in Nolan et al. (2012). We used the best fit positions obtained through `pointlike` and performed a spectral analysis using `gtlike`.

After fitting the position of a source, we use `gtlike` to perform a likelihood-ratio test for the detection of the source. Here, TS is defined as

$$\mathrm{TS} = 2\log(\mathcal{L}_{\mathrm{pt}}/\mathcal{L}_{\mathrm{bg}}) \tag{1}$$

where $\mathcal{L}_{\mathrm{pt}}$ is the Poission likelihood for a model including the source and $\mathcal{L}_{\mathrm{bg}}$ the likelihood for a model not including the source. We set the threshold for detection of signfiicant emission at $\mathrm{TS} > 25$, corresponding to a significance just over 4σ (Abdo et al. 2010a).

For the significantly-detected source, after fitting the position of the source we test to see if the spectrum of the source is significantly cutoff following the description in Ackermann et al. (2011). After fitting the source using `gtlike` with both a power-law and exponentially-cutoff spectral model, we define the likelihood ratio test for the cutoff test as From `gtlike`, we obtained

$$\mathrm{TS}_{\mathrm{cutoff}} = 2\log(\mathcal{L}_{\mathrm{cutoff}}/\mathcal{L}_{\mathrm{pt}}) \tag{2}$$

where $\mathcal{L}_{\mathrm{cutoff}}$ is the poisson likelihood for a model including the source with a cutoff spectral model. We set the threshold for detecting a significant cutoff at $\mathrm{TS}_{\mathrm{cutoff}} > 16$, corresponding to a 4σ detection (Ackermann et al. 2011) .

We used `pointlike` to test whether the observed emisssion was spatially extended, assuming a radially-symmetric Gaussian spatial model. `pointlike` can simulatenously fit the position and the extension of the assumed Gaussian source, following the description in (Lande et al. 2012). After the extension fit, we refit the spectrum of the spatially extended source using `gtlike` and performed a likelihood ratio for the significance of the extenstion of a source. Following Lande et al. (2012), we define

$$\mathrm{TS}_{\mathrm{ext}} = 2\log(\mathcal{L}_{\mathrm{ext}}/\mathcal{L}_{\mathrm{pt}}) \tag{3}$$

where $\mathcal{L}_{\rm ext}$ is the Poisson likelihood assuming the source is spatially extended. We set the threshold for detecting the significance of a spatially extended source at $\mathrm{TS}_{\rm ext} > 16$, corresponding to a 4σ detection (Lande et al. 2012).

For sources that are not significantly deteced over the energy range, we compute flux upper limits for the region assuming a fixed spectral index of 2.0. We also computed a pulsed upper limit assuming a canonical pulsar spectrum with an index of -1.7 and a cutoff energy of 3 GeV.

To better assess the spectral charter of any emission in the off-peak region, we performed a spectral analsyis in three smaller energy bins (100 MeV to 1 GeV, 1 GeV to 10 GeV, and 10 GeV to 316 GeV). In each energy bin, we fit the flux and the spectral index of the source. For sources not singificantly detected, we compute a flux upper limit (assuming a fixed spectral index of 2) in the energy bin.

Following the discovery of variable emission from the Crab nebula by the LAT, it is interesting to search for other variable PWN (Abdo et al. 2011). Therefore, we testing all the off-peak regions for variable emission. We divided the 3 year time range into 36 month-long intervals and fit the flux of the source indepnedently in each time range. We compute this significance of the variability using $\mathrm{TS}_{\rm var}$ following the same procedure as the second LAT catalog (Nolan et al. 2012). Since we have 36 months of data, the null distribution (assuming no variability) should follow χ^2 distribution with 35 degrees of freedom, and we set the detection critera for significant variability at $\mathrm{TS}_{\rm var} > 91.7$, corresponding to a 4σ significance detection threshold.

In many situations, this algorithm would fail due to not modeling the position of nearby sources. We expect to be more sensitive to nearby sources than the second LAT catalog both because of our expanded data set (three years of observations instead of two) and also because, for very bright pulsars, we are more sensitivite to other sources once the pulsar has been removed.

Unfortuantly, in many situations, this algorithm failed due to systematics associated with the modeling nearby sources. The large and energy depdended point-spread function of the LAT causes the analysis of any one source to be sensitively affected by the modeling of nearby sources. Therefore, we had to, in many situations, iteratively improve the model of a region by including new sources. This procedure involved generating maps of residual test statistic assuming the presence of a new source (of a fixed spectral index of 2) and looking for regions with $\mathrm{TS} \geq 25$. For these positions, we would include a new source into our model, fit the position and spectrum of this source, and iterate until there was no remaining $\mathrm{TS} \geq 25$ emission.

Even so, there are still some linering regions which have significant emission but which remain particular difficult to model and understand the origion of the emission for. These issues are most likely due to systematics associated with the model of the galactic diffuse emission in the region and issues associated with modeling nearby sources. We will flag these problematic regions in our analysis.

Describe special case of Crab spectrum

1.3. Results

After analyzing the off-peak emission using the pipeline described in § 1.2, we consider any emission in the off-peak region to be magnetospheric in nature if the emsision is not significantly-extended and has a significantly-cutoff spectrum. We consider the emission to originate in the pulsar wind if it is spatially extended or had a hard spectral index. If the source is point-like and had a soft spectrum, or if it is spatially extended but the extension is biased by modeling of the background, we are unable to determine the origin of the emission.

A summay of the reuslts of the pipepline can be found in Table 1. It includes off off-peak phase ranges selected using the method described in § 1.1. This table includes TS, TS_{ext}, and TS_{cutoff} for the significantly detected pulsars (with $TS > 25$). This table also includes the best fit flux and spectral index for these pulsars assuming the best hypothesis (either point-like, spatially-extended, or expontentially cutoff). For the sources that are significantly cutoff, the spectral index refers to the index from the fit of a cutoff spectral model and the final column includes the cutoff energy derived from the fit.

Figure 2 shows the cutoff test...

Consistent with (Abdo et al. 2011), we found the Crab nebula to be highly variable with TS_{var} =XXXX. Besides that, we found no significantly variable off-peak emission. The results of the variability test are contained in the auxiliary information.

The results of the spectral analysis in smaller energy bands described in section § **??** are included in the auxiliary information. In addition, upper limits computed assuming a powerlaw spectral model and a canonical pulsar spectrum are included in the auxiliary information.

Results:

- List of all XXX detections

Table 1. Off-Peak Spatial and Spectral Results

PSR	Phase	TS_{point}	TS_{ext}	TS_{cutoff}	$F_{0.1-316}$ (10^{-9} erg cm^{-2} s^{-1})	Γ	E_{cutoff} (MeV)
J0007+7303	0.53 - 0.89	71.2	10.8	0.0	47.22 ± 8.60	2.61 ± 0.14	···
J0034−0534	0.21 - 0.68	42.8	0.0	4.9	16.82 ± 4.58	2.44 ± 0.16	···
J0101−6422	0.22 - 0.61	25.2	0.0	18.2	45.76 ± 6.41	-5.00 ± 0.00	100.02 ± 1.46
J0102+4839	0.81 - 0.57	69.6	0.0	5.3	26.34 ± 4.89	2.42 ± 0.10	···
J0106+4855	0.67 - 0.03, 0.18 - 0.54	25.5	0.0	0.2	29.14 ± 7.04	2.80 ± 0.17	···
J0218+4232	0.82 - 0.21	50.1	0.0	6.6	55.94 ± 11.20	2.72 ± 0.13	···
J0340+4130	0.13 - 0.64	26.8	0.1	16.5	2.45 ± 1.48	0.93 ± 2.51	645.30 ± 580.54
J0534+2200	0.59 - 0.87	5253.1	0.0	0.0	764.73 ± 18.42	···	···
J0633+1746	0.83 - 0.93	3649.0	2.3	237.3	719.12 ± 27.80	-1.42 ± 0.09	998.24 ± 116.74
J0734−1559	0.28 - 0.84	28.4	10.7	33.4	31.63 ± 6.36	1.77 ± 0.40	100.10 ± 3.01
J0835−4510	0.81 - 0.03	506.0	241.9	0.0	431.14 ± 22.25	2.11 ± 0.03	···
J0908−4913	0.66 - 0.04, 0.17 - 0.54	35.5	9.3	74.1	40.13 ± 37.59	-1.20 ± 0.71	999.01 ± 0.71
J1023−5746	0.67 - 0.03	84.8	57.7	14.1	230.75 ± 6722.99	2.04 ± 0.72	···
J1044−5737	0.55 - 0.97	27.9	187.0	0.0	243.05 ± 2.30	1.95 ± 0.00	···
J1105−6107	0.73 - 0.46	28.9	36.6	78.6	161.16 ± 6644.93	2.14 ± 0.72	···
J1112−6103	0.31 - 0.04	None	None	None	None	None	None
J1119−6127	0.59 - 0.18	40.7	18.3	0.0	54.59 ± 3399.22	2.16 ± 0.70	···
J1124−5916	0.69 - 0.05	86.2	0.0	24.2	26.39 ± 19.44	-0.79 ± 0.72	1000.00 ± 0.71
J1410−6132	0.55 - 0.24	42.4	91.6	12.5	81.41 ± 2783.70	1.79 ± 0.72	···
J1513−5908	0.53 - 0.15	100.6	2.1	0.0	15.83 ± 984.68	1.74 ± 0.72	···
J1620−4927	0.54 - 0.98	27.9	0.5	39.9	72.80 ± 22.94	-0.86 ± 0.25	1000.00 ± 173.04
J1744−1134	0.14 - 0.74	61.4	0.0	15.0	33.38 ± 15.81	2.25 ± 0.09	···
J1746−3239	0.41 - 0.99	53.8	7.2	42.0	61.29 ± 54.13	-1.18 ± 0.71	999.95 ± 0.71
J1747−2958	0.66 - 0.1	53.6	0.0	102.6	146.08 ± 125.15	-1.17 ± 0.71	991.64 ± 0.70
J1801−2451	0.12 - 0.47, 0.6 - 0.96	None	None	None	None	None	None
J1809−2332	0.53 - 0.91	31.5	13.0	15.2	85.80 ± 49.10	2.45 ± 0.11	···
J1813−1246	0.77 - 0.01	57.8	0.0	12.0	147.87 ± 33.22	2.46 ± 0.05	···
J1836+5925	0.76 - 0.92	10450.2	0.0	364.6	497.25 ± 10.72	-1.49 ± 0.02	2024.58 ± 59.89
J2021+4026	0.25 - 0.41	1712.8	37.4	228.3	1248.80 ± 20643.72	2.23 ± 0.72	···
J2043+1711	0.79 - 0.06, 0.18 - 0.55	151.6	0.0	11.9	23.36 ± 9.33	2.18 ± 0.08	···
J2055+2539	0.37 - 0.87	117.0	0.0	30.4	30.05 ± 31.95	-1.45 ± 0.70	999.99 ± 0.71
J2124−3358	0.09 - 0.69	177.7	0.0	27.0	10.88 ± 3.78	-0.61 ± 0.64	1000.01 ± 437.18
J2302+4442	0.75 - 0.23	113.7	0.0	8.4	34.35 ± 5.34	2.36 ± 0.09	···

Note. —

Put table comments

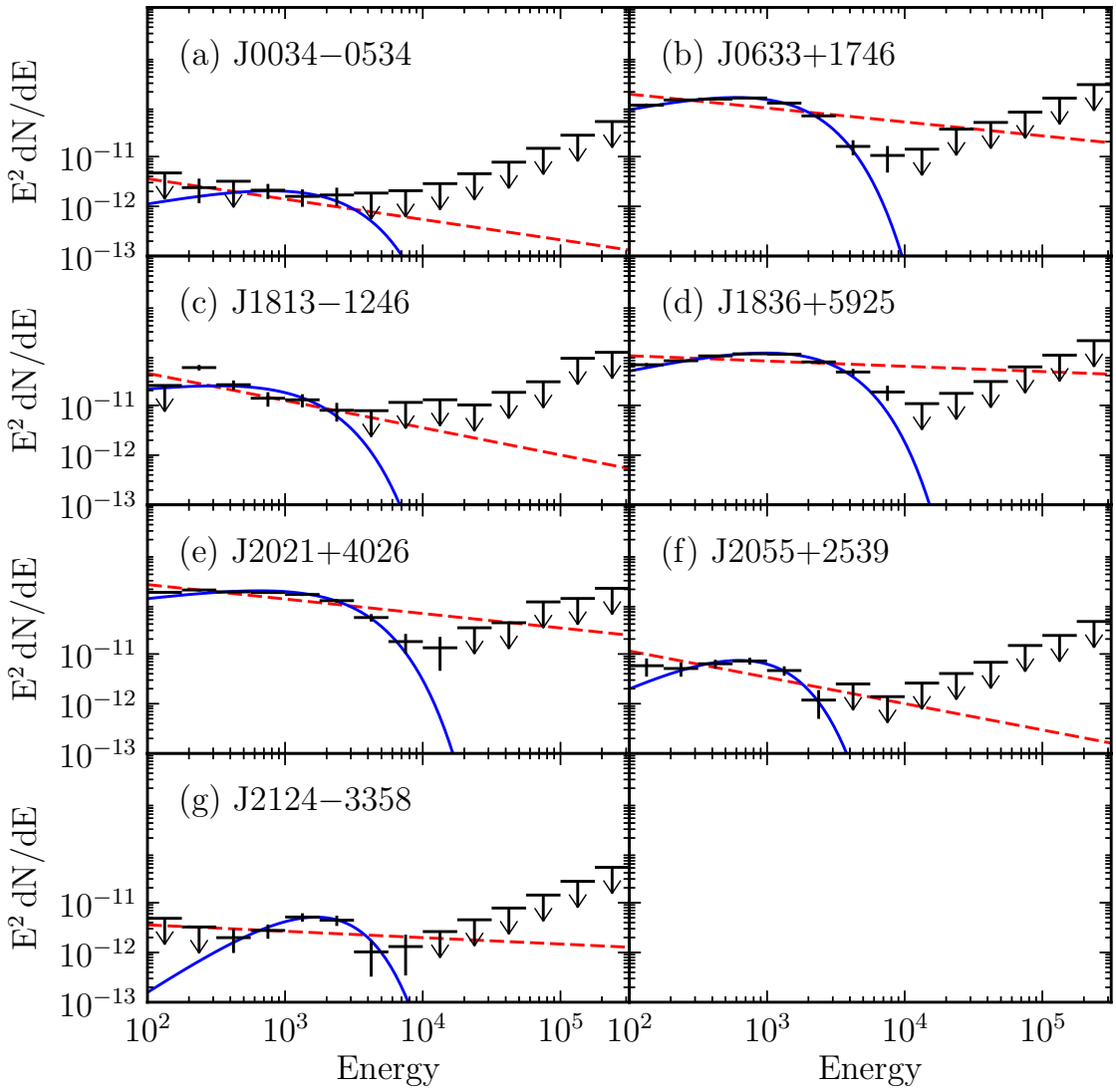

Fig. 2.— Cutoff test for some pulsars...

- For each pulsar, is it a
  - Magnetospheric emission
  - PWN emission
  - Region where the fit shows trouble for some reason.

In our analysis, we detected the the Vela X PWN (associated with PSRJ0835−4510), the Crab Nebula (associated with PSRJ0534+2200), and MSH 15−52 (associated with PSRJ1513-5908).

What to say about PSRJ1023-5746

Sources we detect as clearly magnetospheric

Special cases/problem cases:

- PSRJ0101-6422: Very weird spectrum
- PSRJ1112-6103: Very close to MSH 11 62 (arXiv:1202.3371v1). Nearby source is 2FGL J1112.1-6040. Significant extension.
- When fitting PSRJ1119-6127, description of adding nearby point source to represent emission residual from o represent residual from PSRJ1112-6103 looking spatially extended.
- PSRJ1418-6058 and PSRJ1420-6048, very difficult to analyze because both very near eachother.
- Something about the complciated Gamma Cygni PSR: PSRJ2021+4026
- PSRJ1105-6107: something about adding source to background model that is very nearby. .
- PSRJ1648-4611 (what to do about nearby 2FGL soruce and other residual emission. Is this paper relevant: http://arxiv.org/pdf/1111.2043.pdf???)?
- What to do about emission from PSR J1023 at low energy???
- PSRJ0908-4913: waht to say about far localization?

See what OZLEM is doing

Describe how we present the point-like hypothesis for signifciant extended soures if the extension fails for some reason

1.4. Discussion

Maybe a pulsar physics person can fill in this discussion.

REFERENCES

Abdo, A. A., et al. 2010a, ApJS, 188, 405

—. 2010b, ApJ, 708, 1254

—. 2011, Science, 331, 739

Ackermann, M., et al. 2011, ApJ, 726, 35

Ackermann, M., et al. 2011, ApJ, 726, 35

Grondin, M.-H., et al. 2011, ApJ, 738, 42

Jackson, B., et al. 2005, IEEE, Signal Processing Letters, 12, 105

Lande, J., et al. 2012, ApJ, in preparation

Nolan, P. L., et al. 2012, ApJS, 199, 31

A. Description of Auxiliary information for Off-peak Analysis

A more complete list of the results from the pipeline are contained in a supplimental `fits`-format table.

Here, we describe each column contained in the fits table:

- Column `TS_point` is the test statistic obtained at the best fit position of the assumed point-like source
- Column